

Numerical Analysis of Small Movable ICRF Antenna Loading Resistance in Heliotron-E

OKADA Hiroyuki*, KOTANI Tadashi¹, MUTOH Takashi², SANO Fumimichi, KONDO Katsumi³,
WAKATANI Masahiro³ and OBIKI Tokuhiko

Institute of Advanced Energy, Kyoto University, Uji 611-0011, Japan

¹*Faculty of Engineering, Kyoto University, Kyoto 606-8501, Japan*

²*National Institute for Fusion Science, Toki 509-5292, Japan*

³*Graduate School of Energy Science, Kyoto University, Uji 611-0011, Japan*

(Received: 30 September 1997/Accepted: 12 January 1998)

Abstract

In order to study the dependence of the angle between the antenna RF current and the magnetic field line on the plasma loading resistance in Ion Cyclotron Range of Frequency (ICRF) heating, a small loop antenna was fabricated and introduced into Heliotron-E device. The loading resistance decreased gradually with the distance between the antenna and the plasma edge as expected. When the antenna was rotated, the loading resistance became very large value unexpectedly at the angle near 70 degrees between the antenna and the magnetic field. To understand the result, we developed the numerical code including the magnetic field direction in the model of the calculation. The angular dependence from the calculation has broader peak than that observed in the experiment.

Keywords:

ICRF, antenna loading resistance, loop antenna, variational analysis, Ritz's method

1. Introduction

In ICRF heating experiments in Heliotron-E, the effective ion heating and the fast ion production were achieved [1, 2]. But the antenna loading mechanism is not so clear because of its strong shear especially near the edge region [3]. To study the relation of the angle between the antenna RF current and the magnetic field line, and heating mechanisms, a small loop antenna was fabricated. It was introduced into Heliotron-E through the outer horizontal port. It can be moved horizontally, rotated around the central feeder structure. The angle between the antenna and the central feeder is changeable as well. The central conductor is covered by Faraday shield to cancel the electric field perpendicular to the RF current.

The antenna impedance for the coupling efficiency of RF power is measured by the current pickup loop

and the voltage probe in the transmission line between the antenna and the matching circuit. When we rotated the single antenna keeping the distance from a plasma, the antenna loading resistance increased at about 70 degrees of the angle between the magnetic field line and the antenna current. The width of the resistance peak was not so large.

For understanding this result, we made numerical calculation code based on Theilhaber's paper [4]. For the fast wave heating analysis, $E_{\parallel} = 0$ approximation is usually adopted. However, to evaluate the coupling of another mode related with E_{\parallel} , for example, ion Bernstein mode, the additional terms must be taken into account in Maxwell equations. The angular dependence of the loading is contained in this code in order to compare the experimental results.

*Corresponding author's e-mail: okada@center.iae.kyoto-u.ac.jp

2. Model and Boundary Conditions in the Numerical Analysis

A plasma is treated in the slab geometry shown in Fig. 1. The antenna loop is defined as three dimensional structure. The quantities in the y - and z -coordinates are Fourier transformed in the calculation. The magnetic field line is fixed in z -direction. For the model in Ref. [4], the antenna current is normal to the magnetic field line. In our code, the antenna loop can be rotated in y - z plane. The antenna current is assumed to flow in y' direction shown in Fig. 2. The perpendicular direction to y' is defined as z' . When the angle between the antenna current and the magnetic field line is 90 degrees, y and y' , z and z' are identical, respectively.

The voltage source is assumed to be located at the connection edge of the antenna. The other side is short circuited to the wall. The position of the voltage source is considered to be $(x, y) = (0, -h)$ as in Fig. 1. Then,

$$E^{\text{ext}}(R) = \hat{e}_x V_a \delta(x), \quad (1)$$

where R denote to the edge area of the antenna. The induced electric field E^{ind} by external field E^{ext} is as follows,

$$E_T^{\text{ind}}(R) + E_T^{\text{ext}}(R) = 0. \quad (2)$$

The suffix T represents the tangential component along the antenna central conductor. E^{ind} is assumed to be proportional to the integrated current along the conductor. Antenna impedance Z_a is represented as follows,

$$Z_a = \frac{\int_D dR K(r) \cdot \mathcal{L}^{\text{op}} \cdot J(R)}{\int_D dR K(R) \cdot \mathcal{M}^{\text{op}} \cdot J(R)}, \quad (3)$$

where J is antenna current, K is any current for using the variational principle, \mathcal{L}^{op} is the tensor determining the induced electric field from the current and \mathcal{M}^{op} is the tensor of the external electric field from the current respectively.

The boundary conditions for the electric field are summarized below.

$$E_z(0) = 0, \quad (4)$$

$$E_y(c) \sin \theta - E_z(c) \cos \theta = 0, \quad (5)$$

$$\begin{aligned} & \frac{d}{dx} E_z(b + \varepsilon) - \frac{d}{dx} E_z(b - \varepsilon) \\ &= i(n_z^2 \sin \theta + n_y n_z \sin \theta - \sin \theta) J_y \\ &- n_z J_x, \end{aligned} \quad (6)$$

$$E_z(b + \varepsilon) = E_z(b - \varepsilon). \quad (7)$$

All quantities are normalized and Fourier-transformed in y and z directions as in Ref. [4]. ε is a small parameter. n_y and n_z are normalized wave number in y and z directions, respectively. Equation (4) is due to the assumption of the perfect conductor wall. Equation (5) is

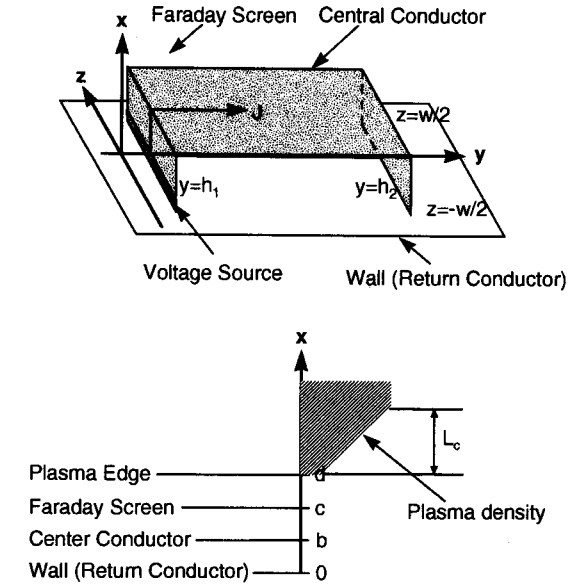


Fig. 1 Antenna model in the numerical analysis of the antenna impedance.

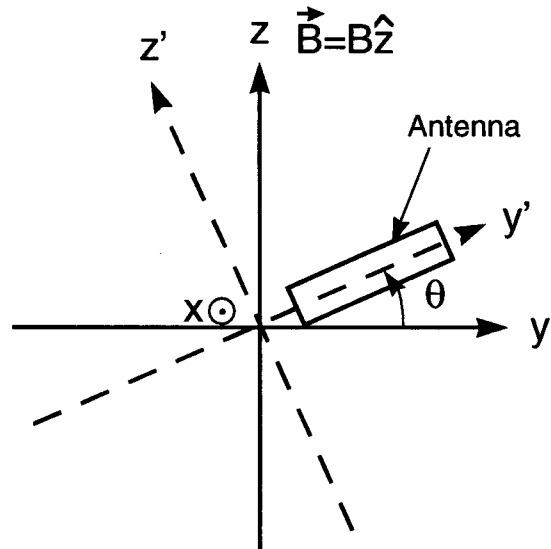


Fig. 2 The definition of the rotation angle θ and the coordinates used in this calculation.

derived from the existence of the screen at $x = c$. The third condition is obtained by the integration of the transmission equation. The last one is derived according to Stokes s theorem.

The boundary conditions for the magnetic field are obtained similarly,

$$\frac{dH_z(0)}{dx} = 0, \quad (8)$$

$$H_z(b - \varepsilon) \cos\theta - H_y(b - \varepsilon) \sin\theta - H_z(b + \varepsilon) \cos\theta + H_y(b + \varepsilon) \sin\theta = J_y(b), \quad (9)$$

$$\frac{dH_z(b + \varepsilon)}{dx} - \frac{dH_z(b - \varepsilon)}{dx} = 0, \quad (10)$$

$$H_z(d) = - \frac{1}{Z_p(1 - n_z^2)} \left[n_y n_z E_z + i \frac{dH_z}{dx} \right]_{x=d}, \quad (11)$$

where $Z_p (= E_y/H_z)$ is impedance at the plasma edge ($x = d$). The procedure of determining this value is as follows. First, H_y and E_z at the given point near the resonance are calculated using WKB method assuming the outgoing wave condition. Then, Z_p is obtained resolving the Maxwell equations with the dielectric tensor in a plasma.

3. The Experimental and Calculated Results

The impedance of the antenna is observed in the experiment using the signals of the directional couplers, the voltage probe and the current pickup coil. The result is shown in Fig. 3 with calculated values. The plasma parameters of the experiment are as follows,

- line averaged electron density: $2.0 \times 10^{19} \text{ m}^{-3}$,
- central electron temperature: 400 eV,
- central ion temperature: 60 eV,
- minority proton ratio (H/D plasma): 0.15,
- magnetic field strength on axis: 1.9 T.

The frequency of the ICRF wave is 26.7 MHz. Antenna length is 0.276 m and its width is 0.07 m. The plasma edge position in Fig. 3 corresponds to the origin of the abscissa. Each value represents net plasma loading resistance because the vacuum resistance is already subtracted. The vacuum resistance is about 0.3 Ω . The dependence for the distance between the plasma edge and the antenna agrees in the experimental error except absolute magnitude. The calculated value is about one fifth of the experimental one. Because the return conductor of the antenna is not contacted with the chamber wall, the radiation area of the antenna loop seems to increase effectively. This fact causes the increment of

the resistance.

The angular dependence of the antenna current against the magnetic field line is shown in Fig. 4. The antenna was rotated keeping the fixed distance between a plasma and the antenna. Around 70 degrees, the resistance becomes large. In this figure, the calculation result is also indicated. The calculated values have very broad dependence against the antenna current angle. Because the antenna crosses the ion cyclotron layer in the neighbor of 90 degrees, the large resistance near 90 degrees is expected. The resistance peak shifted from the 90 degrees cannot be explained by the numerical

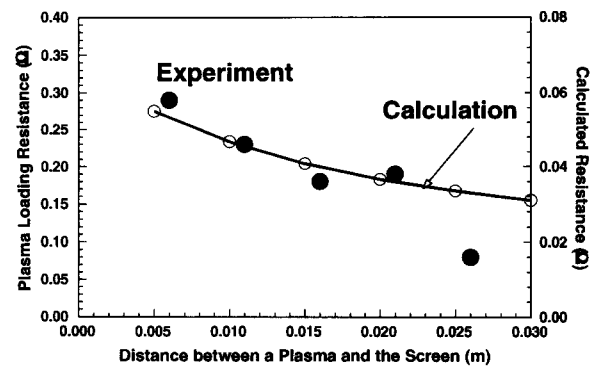


Fig. 3 The plasma loading resistance from the experiment (solid circle) and the numerical calculation (open circle and line) vs. the distance between the plasma edge and the antenna Faraday screen. The scale of the ordinate for the calculation is five times larger than that of experiment.

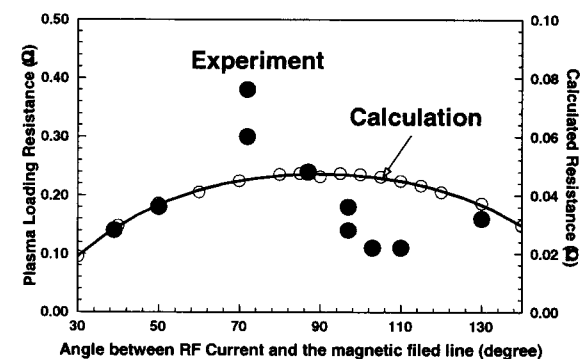


Fig. 4 The plasma loading resistance from the experiment (solid circle) and the numerical calculation (open circle and line) vs. the angle between the antenna current and the magnetic field line. The difference of the scale of the ordinates between calculation and experiment is the same as that in Fig. 3.

analysis. The angle along the antenna loop changes within several tens degrees because of the large rotational transform and the shear of Heliotron-E magnetic field. This effect is not included in the calculation. It may cause the different angular dependence.

4. Summary

In order to understand the dependence of the loading resistance of ICRF antenna in Heliotron-E, we developed the numerical code which can analyze the dependence of the angle between the antenna current and the magnetic field line. The change of the angle of the magnetic field line along the ICRF antenna loop must be included in the calculation in the future.

Acknowledgment

The authors would like to thank the Heliotron-E group for operating the Heliotron-E device.

References

- [1] T. Mutoh *et al.*, Nucl. Fusion **24**, 1003 (1984).
- [2] H. Okada *et al.*, Nucl. Fusion **36**, 465 (1996).
- [3] K. Uo *et al.*, *Plasma Physics and Controlled Nuclear Fusion Research, 1980 (Proc. 8 Int. Conf. Brussels, 1980)*, Vol.1, IAEA, Vienna, p.217 (1981).
- [4] K. Theilhaber *et al.*, Nucl. Fusion **24**, 541(1984).